Excess Heat Capacity in Mo/Au Transition Edge Sensor Bolometric Detectors

A. D. Brown, R. P. Brekosky, F. Colazo-Petit, M. A. Greenhouse, J. P. Hays-Wehle, A. S. Kutyrev, V. Mikula, K. Rostem, E. J. Wollack, *Senior Member, IEEE*, and S. H. Moseley

***Abstract*—Excess heat capacity in a bolometric detector has the consequence of increasing or leading to multiple device time constants. The Mo/Au bilayer transition edge sensor (TES) bolometric detectors intended for the high resolution mid-infrared spectrometer (HIRMES) have two response time, one of which is a few times longer than that estimated from materials used in the design. The relative contribution of this settling time to the overall time response of the detectors is roughly proportional with the pixel area, which ranges between ~0.3 and 2.6 mm^2. Use of laser ablation to remove sections of the silicon membranes comprising the pixels results in a detector response with a smaller contribution from the secondary time constant. Additional information about the nature of this excess heat capacity is gleaned from glancing incidence x-ray diffraction, which reveals the presence of molybdenum silicides near the silicon surface from the bi-layer deposition. Quantitative analysis of the concentration of excess molybdenum, estimated with secondary ion mass spectroscopy, is commensurate to the additional heat capacity needed to explain the anomalous time response of the detectors.**

***Index Terms*— Microfabrication, superconducting photodetectors, surface contamination, thin film sensors.**

I. Introduction

THE high resolution mid-infrared spectrometer (HIRMES) was slated to be a facility-class instrument for the stratospheric observatory for infra-red astrophysics (SOFIA). HIRMES was designed to probe several important aspects of protoplanetary formation by providing low (~600) to very high (~100,000) spectroscopy in the 25-122 micron spectral regime [1].

Central to the HIRMES instrument were its two types of high filling fraction detector arrays [2, 3]: One was comprised of two 32x16 sub-arrays of 1 mm x 1 mm transition edge sensor (TES) pixels with a filling fraction of 84.7% in the spectral direction and 99.0% in the spatial direction, and the other was comprised of an 8x16 detector array of TES with eight rows of pixels of different dimensions for each row and a filling fraction ranging between 97.6% and 99.3% in the spatial direction for the smallest and largest pixels, respectively.

Two requirements for the latter, high resolution, detector pixels are a noise equivalent power (NEP) ~ $3x10^{-18}$ W/rt(Hz) and a response time ~5 ms. With a simple thermal model [4], the effective response time of a transition edge sensor (TES) bolometric detector $t_{eff} = t_0/(1+P\alpha/GT)$, where P is the bias power of the voltage biased TES, and α is the steepness of the transition region and is defined as T/R dR/dT, where T is temperature, R is the TES resistance, and $t_0 = C/G$, where C is the heat capacity and G is the thermal conductance between the TES and bath, is the natural time constant. Thus, in the absence of an excess heat capacity, the time response of a TES bolometer is linearly proportional to its heat capacity.

Initial development of the high resolution detectors for the HIRMES instrument involved their fabrication on low stress silicon nitride membranes. Unfortunately, the HIRMES detectors fabricated on silicon nitride membranes had much higher effective time constants (hundreds of ms) than expected, and the excess heat capacity of silicon nitride was believed to be the primary contribution. In fact, it is documented in the literature that silicon nitride has been found to have heat capacity that is much higher than the Debye model estimate. One group [5] attributes this excess heat capacity to the presence of surface micro-states, and another [6] posits that two-level systems are responsible for this anomaly.

On account of the long time constants exhibited by the silicon nitride devices, a decision was made to abandon use of this material as a substrate. Subsequent detector development was undertaken on single crystal silicon substrates. Unexpectedly, these detectors also had much higher than expected time constants, and, in this manuscript, a discussion of possible sources

Manuscript receipt and acceptance dates will be inserted here. Funding was provided by National Aeronautics and Space Administration, Grant No. NNH15ZCA001N-S3GI. *(Corresponding author: Ari Brown.)*

A. D. Brown is with NASA Goddard Space Flight Center, Greenbelt, MD 20771, USA (e-mail: ari.d.brown@nasa.gov).

R. P. Brekosky was with SSAI, Lanham, MD 20706 USA. He is now with NASA Goddard Space Flight Center, Greenbelt, MD 20771, USA (e-mail: regis.p.brekosky@nasa.gov).

F. Colazo-Petit is with Teltrium Solutions, LLC, Rockville, MD 20852 USA (e-mail: felipe.a.colazopetit@nasa.gov).

M. A. Greenhouse is with NASA Goddard Space Flight Center, Greenbelt, MD 20771, USA (e-mail: matt..greenhouse@nasa.gov).

J. P. Hays-Wehle is with the University of Maryland, Baltimore County, Baltimore, MD 21250 USA (e-mail: james.p.hays-wehle@nasa.gov).

A S..Kutyrev is with the University of Maryland, College Park, College Park, MD 20742, USA (e-mail: alexander.s.kutyrev@nasa.gov).

V. Mikula is with the American University, Washington, DC 20016 USA (e-mail: vilem.mikula-1@nasa.gov).

K. Rostem is with the University of Maryland, Baltimore County, Baltimore, MD 21250 USA (e-mail: karwan.rostem@nasa.gov).

E. J. Wollack is with NASA Goddard Space Flight Center, Greenbelt, MD 20771, USA (e-mail: edward.j.wollack@nasa.gov).

S. H. Moseley was with NASA Goddard Space Flight Center, Greenbelt, MD 20771, USA. He is now with Quantum Circuits, Inc., New Haven, CT 06511, USA (e-mail: samuel.h.moseley@nasa.gov).

Color versions of one or more of the figures in this paper are available online at http://ieeexplore.ieee.org.

Digital Object Identifier will be inserted here upon acceptance.

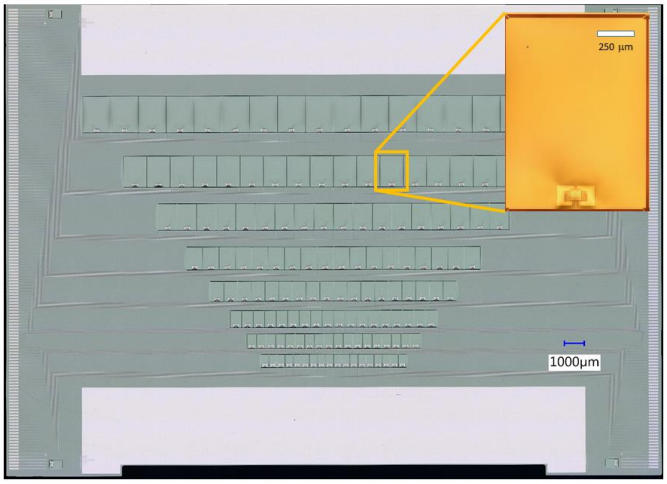

Fig. 1. Stitched micrograph of a HIRMES high resolution detector array.

and means to mitigate excess heat capacity on Mo/Au TES bolometric detectors fabricated on silicon membranes is provided.

II. HIRMES High Resolution Detectors

Figure 1 shows a micrograph of a HIRMES high resolution detector array. There are eight 1x18 detector pixel arrays, in which the central 16 pixels of each array can be read out. The pixels are fabricated on 450 nm thick Si(001) substrates, which are suspended with 5 micron wide x 30 micron long thermal isolation structures. The TES are comprised of Mo/Au bilayer thin films with a superconducting transition temperature Tc~110 mK and are read out via superconducting Nb leads. Additional components of the detector pixels include Ti/Au "heat-sinking" structures contacting the TES at two corners, which are used to engineer the pixel heat capacity, and NbTiN absorber coatings [7, 8], which coat the entire surface of the membrane on the side opposite the TES and which have AlN strain matching and Al2O3 stress compensating layers. Additional details regarding the fabrication of these detectors are provided in Ref. 3.

The largest pixels measure 1.40 mm x 1.84 mm and are, thus, ~2.6 times larger than the largest leg-isolated single pixel silicon bolometers fabricated at NASA Goddard [9]. As discussed later in this manuscript, the contribution of bulk impurities distributed within the silicon membrane, coupled with a large pixel size, resulted in an excess heat capacity, which was several orders of magnitude greater than the Debye estimate of the silicon heat capacity.

III. High Resolution Detector Temporal Response

The detector and time-domain multiplexing (TDM) chips were packaged and cooled in a cryogenic free system that reaches ~70mK using an adiabatic demagnetization refrigerator. Detector arrays were readout using TDM based upon superconducting quantum interference device (SQUID) electronics [10]. The detector signal is further amplified by a SQUID series array stage placed at 3K. The warm readout electronics is made by the University of British Columbia and referred to as a Multi-Channel Electronics (MCE) box. The detector signal is sampled at a rate of 4167 Hz. A square waveform with a 2 sec period is added to the DC TES bias signal to excite the electro-thermal circuit and measure the pixel response functions. The amplitude of the square wave is less than 0.05% of the DC bias value.

IV. Identification of a Root Cause and Mitigation Approaches

From the measurements taken and described in Section 3, it was hypothesized that the root cause of the additional time constant was a dangling heat capacity [11]. Some possible sources of this dangling heat capacity were either: (1) The Ti/Au heat-sinking structures, which may have been weakly thermally coupled to the TES through a superconducting Nb joint, or, (2) one or more layers of surface contamination.

In order to evaluate the contribution of the former, we laser ablated the Ti/Au heat-sinking structure – TES *overlap region* on some pixels, shown in Figure 2(a), and removed both of the Ti/Au heat-sinking structures and the underlying silicon membranes on others. Figure 2(b) shows the time response of a pixels in which the overlap region was laser ablated. The time response of the modified pixel, which has a second pole and is shown in red, is largely unchanged relative to that on another, unmodified, pixel with the same surface area. A similar effect is seen on pixels, which had both of the Ti/Au structures as well as the underlying silicon substrate removed; whereas the first,

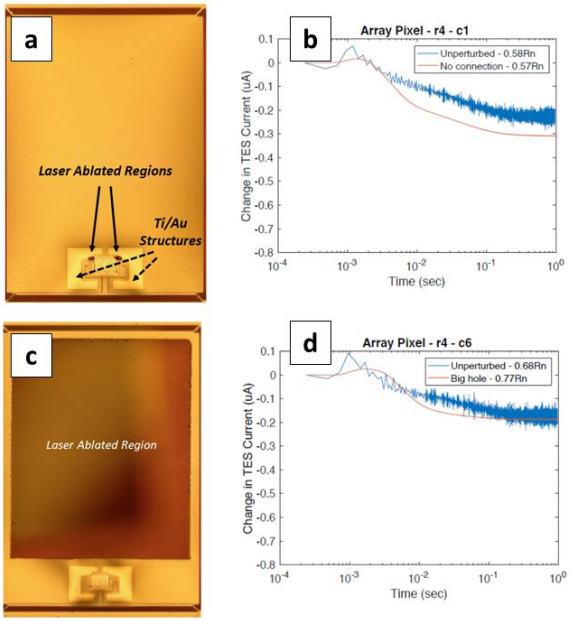

Fig. 2. (a) Image of a detector pixel, in which the Ti/Au heat-sinking structure/TES overlap regions were laser ablated. (b) Time response of the pixel after laser ablation (red curve), illustrates that there are multiple decay times. (c) Image of a detector pixel in which the central region of the detector pixel has been laser ablated. (d) Time response reveals that the second time constant has largely been eliminated. In both (a) and (c), the pixel dimensions are 0.68 mm x 0.98 mm.

natural time constant is smaller in these cases, the weight of the second time constant was not appreciably impacted. As an

aside, it is worth noting that the superconducting transition temperature, saturation power, and transition shape were unaltered by laser ablating regions only tens of microns away from it.

We further exploited the ability to laser ablate regions to identify the location of the dangling heat capacity on the pixels. One modification to certain pixels consisted of ablating regions near the pixel perimeter. This modification resulted in no appreciable change to the detector's time response, and was in disagreement with one hypothesis, in which condensation of fluoropolymers formed during the reactive ion etching process, used to define the membranes, contributed to excess heat capacity.

Another modification consisted of ablating the central portion of the pixel, in which 73% of the membrane was removed (see Fig 2(c) and (d)). This modification resulted in a sharp decrease in the weight of the second time constant. Thus, it was inferred that the source of the excess heat capacity resided either on the silicon surface or within its bulk.

In order to look for the presence of surface contamination, scanning electron microscopy (SEM) was performed. Conventional electron microscopy, using an electron voltage of 10 kV, did not reveal any contamination. However, by using low voltage electron microscopy, with voltage $\leq$ 5 keV, a layer of residue resided near the perimeter of some pixels was observed. Because this residue could not be imaged at higher voltage, it was believed that the residue was organic in nature. This led to the application of a cleaning process demonstrated to remove organic residues on the detector pixels. The process consisted of a succession of intense UV-light exposure, immersion in a commercially available organic base, and oxygen plasma ashing in a reactive ion etcher. After cleaning the pixels, the residues could no longer be seen in the SEM. Furthermore, and more importantly, the amplitude and time constant of the second component was reduced by a factor of four.

Whereas the cleaning process reduced a substantial fraction of the dangling heat capacity, it did not fully eliminate it. This suggested that there were contaminants inside the silicon bulk. Regions near the surface of the silicon membrane were probed with glancing incidence x-ray diffraction. Using an incidence angle ~0.2°, which corresponds to an x-ray penetration depth of ~7 nm in silicon [12], evidence of the presence of a molybdenum silicide, Mo_5Si_3, was seen. This result was unexpected, because the estimated amount of interdiffusion between Mo and Si after the Mo was deposited is < 1 nm [13]. Thus, athermal mechanisms may have contributed to implantation of sputtered Mo atoms into the single crystal silicon substrate.

In order to quantify the amount of the molybdenum contaminant in the silicon bulk, secondary ion mass spectroscopy (SIMS) was performed. Although the SIMS cannot accurately provide atomic concentration as a function of depth into the bulk, because of resputtering of the sample's constituent atoms, one can obtain an accurate value of the areal concentration by integrating the volume concentration over the sample thickness.

What is the impact of molybdenum contaminants on the time response of our pixels? From integrating the SIMS-obtained concentration profiles, the molybdenum areal concentration is 1.8×10^{15} atoms/cm,^{2} which, for the largest HIRMES pixels, translates into an excess heat capacity of ~1.4 pJ/K at 0.1 K [14]. This value is approximately 17 times larger than the expected heat capacity of the sum of the heat capacity of all the other components on the pixels. Furthermore, the magnitude of the heat capacity contribution from the excess molybdenum is similar to that extracted from G x t_0. For the fifth-largest pixels, whose dimensions = 0.82 mm x 1.14 mm, the estimated Mo contribution to heat capacity is 0.5 pJ/K at 0.1 K. This value is the same, within error, to G x t_0.

Does the second time constant disappear when the excess Mo is eliminated? We have some evidence of this in two pixels, in which the top ~10 nm of silicon had been, inadvertently, ion milled. Their time response exhibited a single exponential decay, t_{eff} ~2.85 ms.

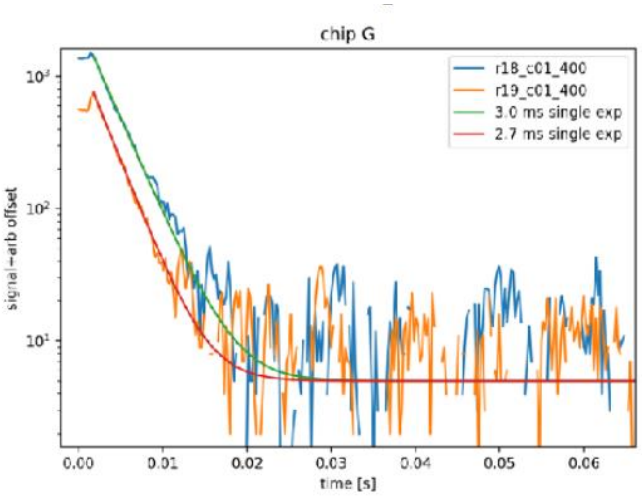

Fig. 3. Time response of two detector pixels after the top 10 nm of silicon substrate had been, inadvertently, been etched. Note the presence of a single pole response.

Therefore, it is quite likely that molybdenum contaminants near surface regions of the silicon membranes are a major contributor to an excess, dangling, heat capacity. Some methods to mitigate or eliminate the presence of the molybdenum contaminants might include use of a lower power Mo sputtering deposition process, depositing the Mo in another manner [15], depositing the Mo through a lift-off mask, or employing a low heat capacity diffusion barrier.

V. Conclusion

High filling fraction TES bolometric detector pixels with Mo/Au TES bilayers deposited on crystalline silicon substrates were found to have two time constants, one of which was much larger than the other and whose weight scaled with pixel area. We attribute this additional time constant to a dangling heat capacity, which takes the form of organic residue and molybdenum atoms embedded in the silicon membrane. We have demonstrated fabrication methodologies to remove both of these contaminants, and future large area and high filling factor bolometric detectors with millisecond time constants may need to follow these methodologies in order to achieve their expected performance.

ACKNOWLEDGMENT

The SIMS characterization of our samples was provided by Eurofins EAG Materials Science.

REFERENCES

1. S. N. Richards, *et al*., "SOFIA-HIRMES: Looking Forward to the HIgh-Resolution Mid-infrarEd Spectrometer," J. of Astronom. Instru., 7 (4), 1840015 (2018), https://doi.org/10.1142/S2251171718400159.
2. E. M. Barrentine, K. Rostem, *et al.*, "Characterization of Si Membrane TES Bolometer Arrays for the HIRMES Instrument," J. of Low Temp. Phys., 193, 241 (2018), https://doi.org/10.1007/s10909-018-1966-4.
3. A. D. Brown, et al., "Fabrication of Ultrasensitive TES Bolometric Detectors for HIRMES," J. of Low Temp. Phys., 193, 675 (2018), https://doi.org/10.1007/s10909-018-1914-3.
4. [4] K.D. Irwin, "An application of electrothermal feedback for high resolution cryogenic particle detection," Appl. Phys. Lett., 66, 1998 (1995), https://doi.org/10.1063/1.113674.
5. M. Kenyon, P. K. Day, C. M. Bradford, *et al.*, "Heat Capacity of Absorbers for Transition Edge Sensors Suitable for Space-Borne Far-IR/Submm Spectroscopy," IEEE Trans. Appl. Supercond., 19 (3), 524 (2009), doi:10.1109/TASC.2009.2017703.
6. [6] M. E. Eckart, *et al.*, "Experimental Results and Modeling of Low-Heat-Capacity TES Microcalorimeters for Soft-X-ray Spectroscopy," AIP Conf. Proc., 1185, 430 (2009), https://doi.org/10.1063/1.3292370.
7. T. M. Miller, *et al.*, "A Path to High-Efficiency Optical Coupling for HIRMES," J. Low Temp. Phys., 193, 681 (2018), https://doi.org/10.1007/s10909-018-1939-7.
8. Brown A. D., Miller, K. H., Wollack, E. J., 2019, Niobium titanium nitride thin film coatings for far-infrared absorption and filtering, US Patent 10458853.
9. D. Benford, *et al*., "5,120 superconducting bolometers for the PIPER balloon-borne CMB polarization experiment," Proc. SPIE, 7741, 77411Q (2010), https://doi.org/10.1117/12.856491.
10. W. B. Doriese, et al., "Developments in Time-Division Multiplexing of X-ray Transition-Edge Sensors," J. of Low Temp. Phys., 184, 389 (2016), https://doi.org/10.1007/s10909-015-1373-z.
11. I. Maasilta, "Complex impedance, responsivity, and noise of transition edge sensors: Analytical solutions for two- and three-block thermal models," AIP Advances, 2, 042110 (2012), https://doi.org/10.1063/1.4759111.
12. K. Omote, "High resolution grazing-incidence in-plane x-ray diffraction for measuring the strain of a Si thin layer," J. Phys. Condens. Matter., 22, 1 (2010), doi:10.1088/0953-8984/22/47/474004.
13. K. Holloway, K. B. Do, R. Sinclair, "Interfacial reactions on annealing molybdenum-silicon multilayers," J. Appl. Phys. 65, 474 (1989).
14. G. R. Stewart, "Measurement of low-temperature specific heat," Rev. Sci. Instru., 54, 1 (1983), https://doi.org/10.1063/1.1137207.
15. F. M. Finkbeiner, J. S. Adams, S. R. Bandler, *et al.*, "Electron-Beam Deposition of Superconducting Molybdenum Thin Films for the Development of Mo/Au TES X-ray Microcalorimeters," IEEE Trans. on Appl. Supercond., 27, 2100104 (2017), doi:10.1109/TASC.2016.2633785.